Natural Hazards (2022) 112:2385–2401
https://doi.org/10.1007/s11069-022-05270-6

ORIGINAL PAPER

Stage-based flood inundation mapping

Robert E. Criss[1] · David L. Nelson[2]

Received: 23 August 2021 / Accepted: 3 February 2022 / Published online: 22 February 2022

Abstract
New methods allow the direct computation of flood inundation maps from lidar data, independently of discharge estimates, hydraulic analysis, or defined cross sections. One method projects the interpolated profile of measured flood levels onto surrounding topography, creating a smooth inundation surface that is entirely based on data and geometrical relationships. A second method computes inundation maps for any simple function that relates the water surface to the elevation of the channel bottom, exploiting their known, sub-parallel character. A final method theoretically combines the elevation of the channel bottom and the upstream catchment area for points along the thalweg, all defined by lidar data. Historical data from stream gauges can be incorporated to generate inundation maps for floods having different return periods. The conceptual simplicity and realism of these maps facilitate data-based planning.

Keywords Inundation mapping · Floods · DEM · Flood recurrence

1 Introduction

The human and economic consequences of flooding range from agricultural benefits to terrific destruction. Efforts to measure and predict flooding began thousands of years ago, as exemplified by the ancient staff gauges called “nilometers” that the Egyptians used for agricultural planning. During the 1800s, the U.S. Army Corps of Engineers established a network of staff gauges along major rivers to facilitate inland navigation (USACE 2020). River stage was of primary interest, although floats and other devices were occasionally used to estimate water velocities and discharge. The number of USACE stream gauges has grown and been augmented by gauges run by the National Weather Service (NWS 2020a) and the U.S. Geological Survey (USGS 2020a, b).

During the 1900s, attention was increasingly directed to the estimation of discharge, which is a useful metric for resource evaluation and scientific studies. Instruments for discharge estimation were improved, and rating curves relating discharge to stage were calibrated at many gauged sites (Wahl et al., 1995). Over time, discharge became

Robert E. Criss
criss@wustl.edu

1 Department of Earth and Planetary Sciences, Washington University, St. Louis, MO 63130, USA

2 470 Columbia Circle, Pasadena, CA 91105, USA

adopted as the primary variable for the analysis of fluvial geomorphology (e.g., Leopold and Marsden 1953) and the prediction of flood-frequency (USGS 1981; USACE 2004). Efforts to quantify federal flood insurance rates fostered the establishment of FEMA in 1979, the development of new statistical methods to calculate flood risk, and the production of maps delineating areas of probabilistic flooding. The latter mapping efforts were primarily based on the HEC-RAS computer program (e.g., FEMA 2015, 2020) that uses discharge as a primary computational variable. Inundation maps are the focus here.

The computational protocols used to produce inundation maps have become increasingly convoluted over time. This paper addresses a circularity that is masked by this complexity. In short, water levels are accurately and continuously measured at gauging stations, then calibrations are made to estimate discharge from those water levels, then the discharge estimates are statistically processed to evaluate probabilistic flooding, and finally these probabilistic discharge estimates serve as essential inputs for the calculation of inundation maps, which depict water levels! The practical and theoretical drawbacks of this circular approach begin with discharge being a computed, dependent quantity rather than a simple measurement, underscoring its problematic use as the primary variable for flood analysis (Criss 2016; Criss and Luo 2017). A second problem with this approach is that errors become progressively magnified in any model based on sequential calculations. Finally, the number of assumptions, empiricisms, and fitting parameters used in HEC-RAS is large compared to the single parameter, water level, of primary interest (Table 1), introducing another theoretical problem (cf. Transtrum et al. 2015).

This paper provides several methods to circumvent this constellation of problems, by computing inundation maps from a direct combination of lidar-based digital elevation maps (DEMs) with observed flood levels, or with a single empirical or theoretical relationship that describes the floodwater surface. Though illustrated for two sites in eastern Missouri, our methods are general and can be applied to many different areas.

2 Hydrogeologic setting

Example maps and calculations will be shown for two sub-basins of the flood-prone, 290 km^2 River des Peres watershed (hereafter, RdP), St. Louis, Missouri. The RdP is located about 25 km southwest of the famous confluence of the Missouri and Mississippi Rivers, in a temperate region of moderate topographic relief bordering the

Table 1 Comparison of HEC-RAS and the methodology proposed here

Method	Inputs	Assumptions	Output
HEC-RAS	DEM data; roughness, expansion and contraction coefficients; bankfull levels; discharge estimates; etc	Energy equation, Manning equation, Interpolation and projection	Inundation map
This paper #1	DEM and flood level data	Interpolation and projection	Inundation map
This paper #2	DEM data	Curve fit and projection	Inundation map
This paper #3	DEM data	Power law and projection	Inundation map

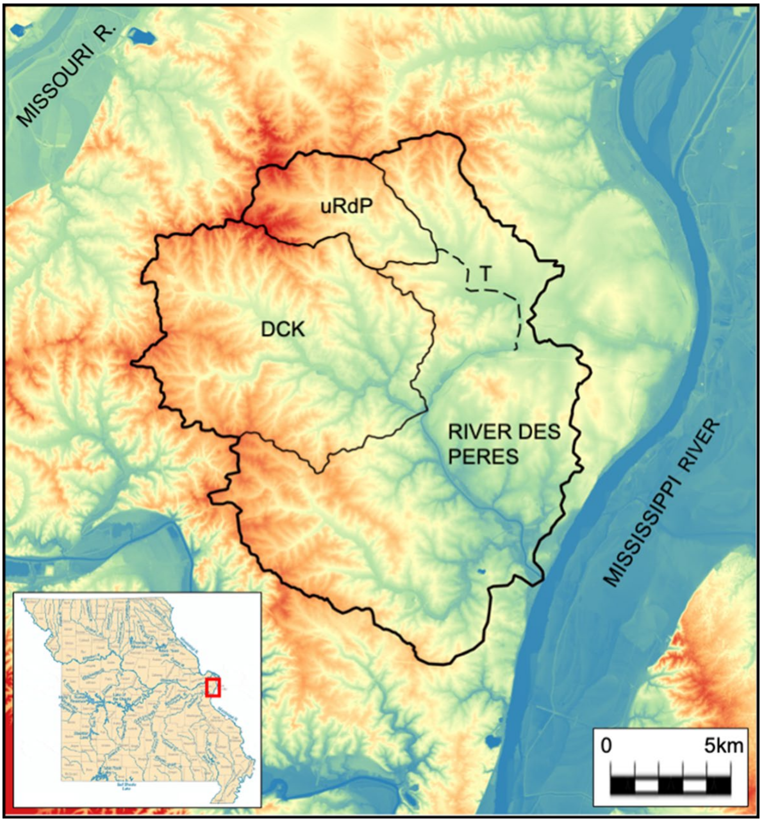

Fig. 1 DEM of the River des Peres watershed, St. Louis, Missouri. Heavy black line delineates the RdP watershed, and the thinner black lines show the upper River des Peres (uRdP) and Deer Creek (DCK) sub-basins. Dashed line is the RdP tunnel (T). Small red rectangle in the inset (lower left) shows the location of this figure in the state of Missouri

Ozarks (Fig. 1; Vineyard 1967). Average annual rainfall in the last 25 years has been 107 ± 21 cm (NWS 2020b), but sharp convective storms that deliver ≥ 4 cm of rain per hour occur during most years (NOAA 2017). Such storms induce flash floods on many St. Louis creeks, which can rise as rapidly as 3 m/h (Criss and Nelson 2020).

The upper River des Peres (uRdP; 25.0 km^2) and Deer Creek (DCK; 95.2 km^2) sub-basins of the RdP are considered in detail below (Fig. 1). The uRdP flows in an open channel that has been straightened and channelized along much of its length, although several reaches with vegetated banks remain. This stream drains into a large tunnel, partly constructed in preparation for the 1904 World's Fair, that was enlarged and lengthened in the 1930s (ASCE 1988). In contrast, most of Deer Creek has vegetated banks and a gravel bottom, although some tributaries have reaches with concrete channels. Both the uRdP tunnel and Deer Creek debauch into the lower River des Peres, a large, rock-lined, trapezoidal channel also constructed in the 1930s, that extends down to its confluence with the Mississippi River (ASCE 1988).

The basin of the upper RdP in University City is 43.5% impervious (Southard 2010), so the stream is highly prone to flash flooding after sharp storms. Peak flows at USGS gauging station 07010022 typically occur within one hour of heavy rainfall. Flooding caused significant damage to University City properties in 2013, 2014, 2019 and 2020, even after dozens of homes were bought out by FEMA following the even higher flood of 2008, which caused two fatalities (e.g., Wilson 2009). Water levels attained during the flood of 1957, modeled below, and the 1915 flood were even higher along the lower reaches.

3 Methods

Detailed, lidar-based DEMs (e.g., USGS 2020c) underlie modern inundation maps. These DEMs define the location of stream channels, the detailed elevation of the surrounding terrain, and watershed boundaries. Available software, including the QGIS open-source, geographic information system (GIS) application, can calculate the upstream areas that contribute flow to every watershed element. For small streams the thalweg and channel bottom elevation are also well-defined by DEMs, but bathymetric data are needed to do this for rivers. This detailed topographic information is then combined with different assumptions, empiricisms, estimates, or data to compute inundation maps. Table 1 summarizes this procedure for the widely used HEC-RAS methodology, and compares it to our new methods, outlined below and detailed in our Supplement, that all utilize QGIS software. Table 2 lists all acronyms used in this paper and the Supplement, for convenient reference.

The Supplement provides links to websites where necessary software, documentation and data can be downloaded and describes specific steps for using QGIS functions to perform prescribed operations. Preprocessing for each of the new methods requires acquiring and preparing the DEM (Supplement Sec. 3.1; hereafter SS3.1), defining channel locations for the largest streams and deriving the up-gradient catchment area or "accumulation area" that contributes flow to each point on the DEM (SS3.2). These steps must be completed before the steps described in Sects. 3.1–3.3 below are executed.

Fundamentally, all that is needed to generate an inundation map is a high-resolution DEM containing the area of interest and a "thalweg data table" (TDT) with columns providing the spatial positions (X and Y) of closely spaced points along the main stem of the stream of interest, the distance (D) along the stream from some initial point upstream, and two columns of elevations, Z_{tb} and Z_{ws}. Column Z_{tb} records the elevation of the stream bottom, and the Z_{ws} values provide the elevation of the flood water surface at each point. The TDT is implemented in QGIS as a vector layer of points that can be displayed on the map window and manipulated by numerous built-in tools.

The list of XY positions can be extracted from the DEM by manually digitizing points along the thalweg, or in some cases can be derived from FEMA data, but a superior list can be generated using the tools available in QGIS. Corresponding values for D and Z_{tb} are also easily generated by QGIS using these tools.

Generating values in the Z_{ws} column is not as straight-forward. Three methods to accomplish this are outlined below and described in detail in the Supplement. The first method relies on flood water levels measured in the field; the other two are based on thalweg bottom elevations and up-gradient catchment areas.

Once the TDT has been populated with Z_{ws} values, QGIS can generate inundation maps by projecting those values throughout the DEM, using a nearest-neighbor gridding

Table 2 Acronyms used in this Paper and the Supplement

ASCE	American society of civil engineers
BotElev	Bottom elevation (raster layer)
DCK	Deer Creek
DEM	Digital elevation model
DrnArea	Drainage area (raster layer)
FDT	Flood data table
FEMA	Federal Emergency Management Agency
GIS	Geographic information system
GNSS	Global Navigation Satellite System
HEC-RAS	Hydrologic Eng. Center's River Analysis System
HUD	Housing and Urban Development
MSD	Metropolitan St. Louis Sewer District
NNGA	Nearest-neighbor gridding algorithm
NOAA	National Oceanic and Atmospheric Admin
NWS	National Weather Service
QGIS	Q Geographic Information System
RdP	River des Peres
TDT	Thalweg data table
uRdP	Upper River des Peres
USACE	United States Army Corps of Engineers
USGS	United States Geological Survey
WSEL	Water surface elevation (raster layer)
Supplement	see https://doi.org/10.1007/s11069-022-05270-6.
CRS	Coordinate reference system
CSV	Comma-separated value (data file type)
DIST	Cumulative distance
IDW	Inverse distance weighting (same as NNGA)
GDAL	Geospatial Data Abstraction Library
GPKG	Geo-package (data file type)
GRASS	Geographic Resources Analysis Support System
HU	Hydrologic units
OSX	The Mac operating system

algorithm (hereafter, "NNGA"). The NNGA algorithm is more efficient if the DEM is clipped to the watershed and the TDT lines are first decimated before gridding is performed.

3.1 New method 1

In cases where flood water levels have been measured at several points along or near the thalweg, Z_{ws} values at every closely spaced point along the thalweg can be estimated by interpolation. The inundation map is then made by projecting those known levels onto the surrounding terrain, using NNGA. Accuracy improves with the number of measured sites, and the result is a realistic, data-based inundation map prepared with minimal assumptions. The method is outlined here; details are provided in SS4.

(1) Construct a second "flood data table" (FDT) containing the several XYZ_{ws} flood level points measured in the field. Find the nearest TDT point to each FDT point, and assign the distance (D) in the TDT, to its nearest point in the FDT. With distances along the stream referenced to the same origin in both tables, we can interpolate the known flood levels in some detail along the thalweg to create the final TDT, augmented with the interpolated Z_{ws} values, that will be used for inundation mapping. Any of several programs can be used to accomplish the interpolation, for example, Excel or KaleidaGraph; SS4 provides an Excel method.
(2) Decimate the TDT vector layer by a factor of 10 or more to reduce the execution time of the NNGA tool.
(3) Create a new raster layer "WSEL1" of flood water surface elevations by projecting the interpolated, Z_{ws} water levels in TDT onto all pixels of the DEM, using a QGIS NNGA tool. The nearest single point was used in our examples, but protocols utilizing multiple points and various weighting powers of their distances can also be used.
(4) Use Eq. 1 in the QGIS 'Raster Calculator' tool to compute a new raster layer of the water depth

$$(WSEL1 - DEM) \tag{1a}$$

and then mask or clip negative values, where the land surface is higher than the water. The resultant raster file represents the inundated area and quantifies the water depth.

A simple modification of this method allows the mapping of a different water surface that is parallel to WSEL1 but consistently higher, or lower, by a desired amount *a*. This is accomplished using a modified equation in the raster calculator to create a new raster file of the water depth:

$$(a + WSEL1 - DEM) \tag{1b}$$

where the new water surface is higher or lower than WSEL1 by *a*. Statistical analysis of historical gauging station can provide values of *a* for hypothetical floods with different return periods, so their areas of inundation can be mapped (see below). If additional data are available, such as data from multiple gauging stations, more complex modifications of Eq. 1a can be made.

3.2 New method 2

In cases where measured flood water levels are not available or are rare, a hypothetical inundation map can be generated by directly calculating the Z_{ws} levels from the TDT file of XYZ_{tb} thalweg points. While this is the least accurate method, it is clearly the simplest. In particular, a column of Z_{ws} values can be added to any spreadsheet of XYZ_{tb} coordinates of points along the thalweg by computing:

$$Z_{ws} = a + bZ_{tb} + cZ_{tb}^2 + \ldots. \tag{2a}$$

where a, b, and c are fitting constants chosen to be realistic, and Z_{tb} is the elevation of the channel bottom. These Z_{ws} values can then be projected throughout the DEM, and the hypothetical inundation map prepared, by following steps 2–4 of Method 1.

Rather than modifying the spreadsheet with Eq. 2a, a highly efficient method of visualizing different hypothetical flood maps can be made by simply generating the TDT in

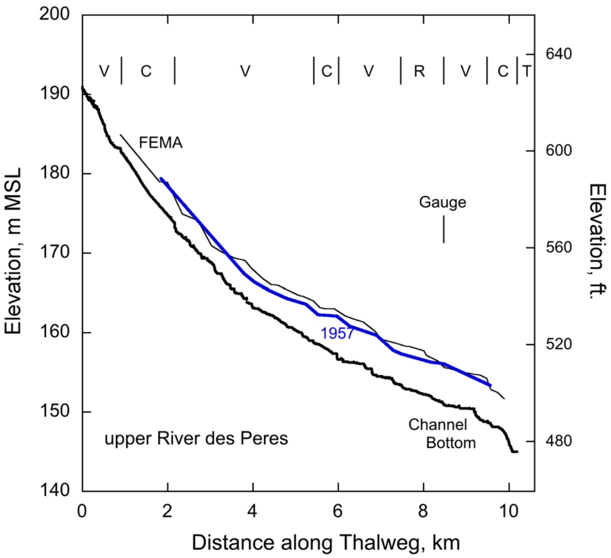

Fig. 2 Profiles of the channel bottom, the interpolated measurements of the 1957 flood level (after Hauth and Spencer, 1971), and the hypothetical, "100-year" base flood (thin upper line; FEMA, 2015) along the upper River des Peres. Channel conditions for various reaches are indicated along the top: C (concrete walls and bottom); V (vegetated banks and gravel bottom); R (trapezoidal rock wall and concrete bottom); T (tunnel). "Gauge" indicates the lateral position of USGS stream gauge 07010022. Note that the flood profiles are sub-parallel to the channel bottom, with increasing water depths downstream

QGIS, and using NNGA to project the channel bottom elevations (Z_{tb} values) onto the DEM. This produces a new raster file "BotElev" that provides the elevation of the channel bottom at the closest thalweg point. Inundation maps can be directly prepared from BotElev by using the QGIS raster calculator to run the following equation, an analogue of Eq. 2a, which will directly produce a new raster file WSEL2 showing hypothetical flood water levels for any indicated choice of *a*, *b* and *c*:

$$a + b * BotElev + c * (BotElev)^2 \tag{2b}$$

Of course, many different types of curves can be used. For a linear fit, *c* is zero, and *b* must be smaller than unity if water depth is to increase downstream, as is the typical condition for real streams; for the two cases we examined, we found $b \sim 0.92$. Equation 2b exploits the reality that thousands of real and computed longitudinal profiles of flood levels are sub-parallel to the channel bottom (e.g., Fig. 2). Moreover, for a given stream, water levels for floods of different recurrence periods are very nearly parallel to each other, so *b* is indeed nearly constant and floods of increasing severity simply have larger values of *a*. As was the case for Eq. 1b, the appropriate value for *a* can be statistically calculated from historical gauge data for any desired return period (see below).

Once the WSEL2 raster file is generated, levels below the actual land surface can be effectively masked, using Eq. 1a with WSEL2 substituted for WSEL1, to create the inundation map.

3.3 New method 3

A theoretical alternative to Method 2 uses the upstream area that contributes overland flow to each point along the channel thalweg, as well as the bottom elevation, to compute the inundation map. The procedure, described in detail in SS5, is summarized here:

(1) In preprocessing, two raster layers are produced: the first contains stream segments ("StreamSegs"), and the second contains accumulated upstream drain areas at every pixel in the DEM ("WaterAccum"). Convert the "StreamSegs" layer to a vector layer, adding a new drain area column (W) to the resulting TDT in the process. The TDT now contains $DXYZ_{tb}W$.
(2) Decimate the TDT vector layer by a factor of 10 or more to reduce the execution time of the NNGA tool.
(3) Next make two new raster layers, one for the channel bottom elevation (BotElev) and one for the drainage area (DrnArea), by projecting Z_{tb} and W respectively onto the surrounding terrain of the DEM, as in step 3 of Method 1.
(4) Finally, use Eq. 3 in the raster calculator to compute a new raster file WSEL3 of flood elevations from layers "BotElev" and "DrnArea":

$$BotElev + b * (DrnArea)^c \tag{3}$$

where b is a fitting constant and c is a power that can range from 0.2 to 0.35, as justified in the next section. Finally, this file is processed using Eq. 1, above, to create the inundation map.

3.4 Power law justification

Theoretical and empirical results provide the basis for Eq. 3. It is well known that, on plots where the logarithm of discharge ($LogQ$) is plotted against the logarithm of drainage area ($LogA$) for streams in a given region, results for the floods of record, for floods of different estimated recurrence times, and for the median annual flood provide strong linear trends of slope j that are nearly parallel, equivalent to the relationship:

$$Q = k_i * A^j \tag{4}$$

where j is a regional constant and the various constants k_i increase with the recurrence interval. Winston and Criss (2016) analyzed data for > 20,000 gauging stations to provide values of j for all physiographic provinces in the conterminous USA. For the Ozarks, they report $j \sim 0.60$, while Southard (2010, Table 5) reports a similar value for urban basins in Missouri.

It is also known that the relationship between water depth H and discharge for numerous gauging stations conforms closely to the "simple rating curve" mentioned in several elementary textbooks:

$$Q = K * H^n \tag{5}$$

where K and n are constants. Criss (2022) determined an average value for n of 2.57 ± 0.64 for 27 long-term gauging stations along the downstream traverse of the Firehole-Madison-Missouri-Mississippi Rivers. Criss and Nelson (2021) analyzed data from 39 gauging stations on small streams near St. Louis, Missouri, finding an average value of 1.82 ± 0.38 for n, and they combined geometric and empirical relationships to show than n should range from about 1.75–3.

Note that discharge Q can be eliminated by equating the right hand sides of Eqs. 4 and 5, providing a direct relationship between water depth H and basin area A for different recurrence intervals:

$$H = \left(k_i/K\right)^{1/n} * A^u \tag{6}$$

where power u is the quotient j/n. It follows that most streams in east central Missouri have $u \sim 0.24$ to 0.34.

3.5 Floods of different recurrence intervals

Values of a in Eqs. 1b and Eq. 2ab, and of b in Eq. 3, are easily adjusted to estimate water levels for floods having different return times. Historical stages of prior floods provide a means to do this in a manner securely grounded in data; such records are available for thousands of stream gauges maintained by NWS, USACE and USGS. These can be used to determine the mean (μ_h) and standard deviation (σ_h) of the list of peak water stages seen in each calendar year (or water year). Statistical stages (h_T) for any recurrence period T (in years) can be calculated from the well-known equation (e.g., Chow, 1964):

$$h_T = \mu_h + K_T * \sigma_h \tag{7}$$

where K_T is an irrational mathematical number that depends on the recurrence interval in years, and the nature of the statistical distribution. For a normal distribution, values of K_T are calculated by solving:

$$T = 2/Erfc\left[K_T/\sqrt{2}\right] \tag{8}$$

For example, for a "ten-year" flood, $K_{10} = 1.28155\ldots$ Values of K_T will differ if the distribution of annual stages is skewed, but values for numerous distributions are tabulated by USGS (1981). Techniques to estimate the appropriate means and standard deviations of records for sites that have undergone temporal changes in conditions are provided by Criss (2016). Finally, differences between values of a in Eq. 1b and 2ab for floods having different return periods are provided by subtracting the appropriate $K_{T\,*}\sigma_h$ factors in Eq. 7.

To estimate parameter b in Eq. 3, the statistical values for local stage h_T must be converted to the statistical water depth H_T, by subtracting the stage h_o that corresponds to the channel bottom:

$$H_T = h_T - h_0 \tag{9}$$

Criss and Nelson (2020) provide several ways to determine h_o at any gauged site.

Finally, estimates for constant "b_T" for any recurrence period can be calculated by equating H_T to the rightmost term of Eq. 3. Rearranging, and using A to represent basin area, provides the quotient:

$$b_T = H_T/A^c = \left(\mu_h + K_T * \sigma_h - h_0\right)/A^c \tag{10}$$

As an example, we estimate the following values for the uRdP: $b_2 = 1.33$; $b_5 = 1.56$; $b_{10} = 1.68$; $b_{25} = 1.81$; $b_{50} = 1.89$; $b_{100} = 1.97$; note that in this calculation, A was entered in km^2 but H and its associated statistical values were entered in meters. Of course, values of b for periods exceeding 25 years involve extrapolation of the data on annual flood peaks, which for this site are available only since 1997. Nevertheless, an independent comparison can be made by comparing the calculation based on Eq. 3 to the values

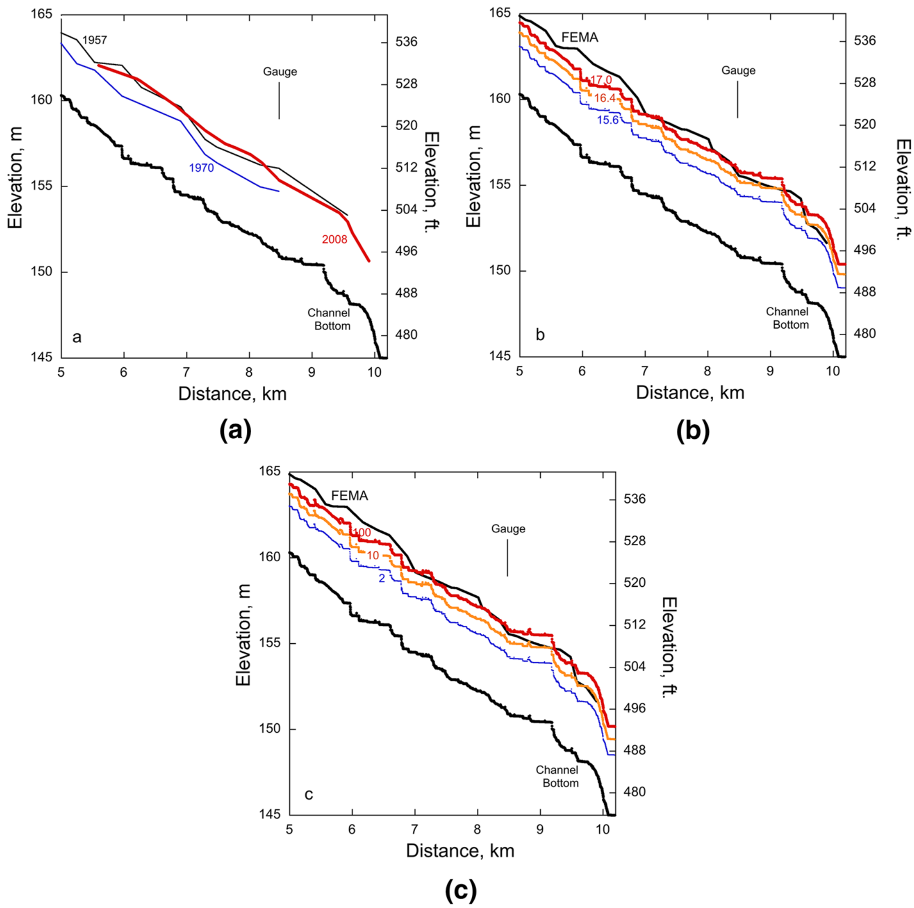

Fig. 3 **a** Real elevation profiles of the channel bottom and the 1957, 1970 and 2008 floods along the upper River des Peres. "Gauge" indicates the lateral position of stream gauge 07010022. **b** Hypothetical flood profiles determined using Eq. 2b, with $c=0$, $b=0.92$ and $a=15.6$, 16.4 and 17.0 m, compared to the FEMA base flood. **c** Hypothetical flood profiles for 2, 10 and 100 year floods computed with Eq. 3, compared to the FEMA base flood. See text

calculated by FEMA (2015); the best match for the region near the gauge is found using $b=1.86$, using a value of 0.3 for power c.

3.6 Example profiles

The panels in Fig. 3 show water surface profiles appropriate for use in Methods 1–3, respectively. These methods can be used to make real or hypothetical inundation maps for any of these profiles, and simple adjustments of the profiles can be used to make additional maps.

Figure 3a shows real profiles for three floods along the upper River des Peres, interpolated between points of measurement. Note that these profiles are nearly parallel and are much smoother than the hypothetical FEMA profile. For comparison, Fig. 3b shows hypothetical profiles calculated with Eq. 2a (Method 2), with numerical coefficients $c = 0$, $b = 0.92$, and values of a determined by the $K_T * \sigma_h$ term of Eq. 7, calibrated with historical data from gauge 07010022 on the upper River des Peres. Finally, Fig. 3c shows profiles for hypothetical floods having different return periods, calculated with Eq. 3 using coefficients stated in the text. Note that all profiles are real in Fig. 3a, but only the channel bottom is real in Figs. 3bc.

4 Results

Example calculations were made for parts of the Deer Creek and uRdP sub-basins. As a first test, Method 1 was used to "reconstruct" the FEMA base flood map in part of the Deer Creek basin, by using FEMA's calculated "base flood" levels at each of their designated cross sections as if they were measured levels for a real flood at various points along the thalweg. Direct comparison of the results with FEMAs inundation map (Fig. 4a) illustrates the accuracy of our computational method. Method 1 was then used to map the inundated area of the 2008 flood, from available measurements along both Deer Creek (Fig. 4b) and the most flood-prone, 4-km long reach of the uRdP (Fig. 5). Criss and Nelson (2020) provide details and references concerning the underlying DEM.

4.1 FEMA base flood

FEMA uses HEC-RAS to estimate the levels of the base flood, commonly called the "100-year" flood, but this actually is a hypothetical flood with a 1% probability of occurring in any given year. Data for St. Louis County are provided by FEMA (2015). Maps 29189C326K and 29189C327K show the relevant part of the Deer Creek basin, while 29189C211K and 29189C212K depict FEMA's results for University City. FEMA (2015; Vol. 1 Table 12) provides their calculated base flood elevations at each of their defined cross sections along these streams, and the data are also available as downloadable shape files.

As a first test of our algorithms, a column indicating the flood elevations calculated by FEMA was added to our table of XYZ_{tb} thalweg positions, at each intersection of the various FEMA cross sections and the thalweg. The column was completed by linear interpolation between the successive cross sections, and then the table was thinned to include results only every 20 m along the thalweg. Those results were projected onto the surrounding region of the DEM, using the NNGA algorithm of QGIS described in Method 1 above, to prepare an inundation map. Our results compare closely with the area of base flood inundation, as mapped by FEMA (Fig. 4a).

4.2 2008 flood, Deer Creek

The flood of record in the RdP basin occurred in 2008, at all but the lowermost gauge which is influenced by backwater from the Mississippi River. Numerous flood marks were

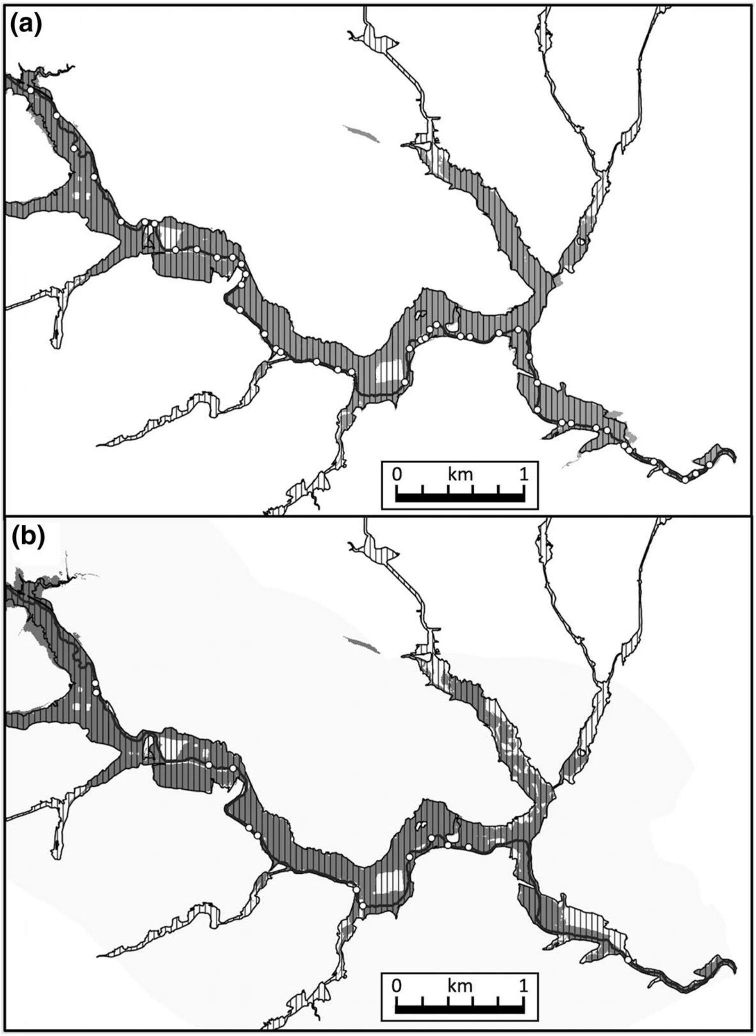

Fig. 4 **a** (Top) Map showing good agreement between the inundated area calculated by Method 1 (gray shading) for lower Deer Creek, compared to the area inundated by the FEMA base flood (vertical ruled pattern). White dots indicate intersections of the thalweg with the cross sections defined by FEMA, where FEMAs hypothetical base flood levels were used in lieu of real flood marks (see text). **b** (bottom) Inundation area of the 2008 flood (gray shading), determined from IDW processing of actual flood marks, per Method 1. Ruled area is Zone AE on FEMA maps, representing the area inundated by the hypothetical, 1% base flood. White dots are sites where 2008 flood elevations were measured, most representing data from MSD (2013)

measured by the Metropolitan St. Louis Sewer District shortly after this event (MSD, 2013). The peak flood level was also recorded at USGS gauging station 07010086, but the other gauges along Deer Creek were either disabled or off-scale during the event. Figure 4b shows our computed inundation map for the area where flood level measurements are most abundant, determined using Method 1.

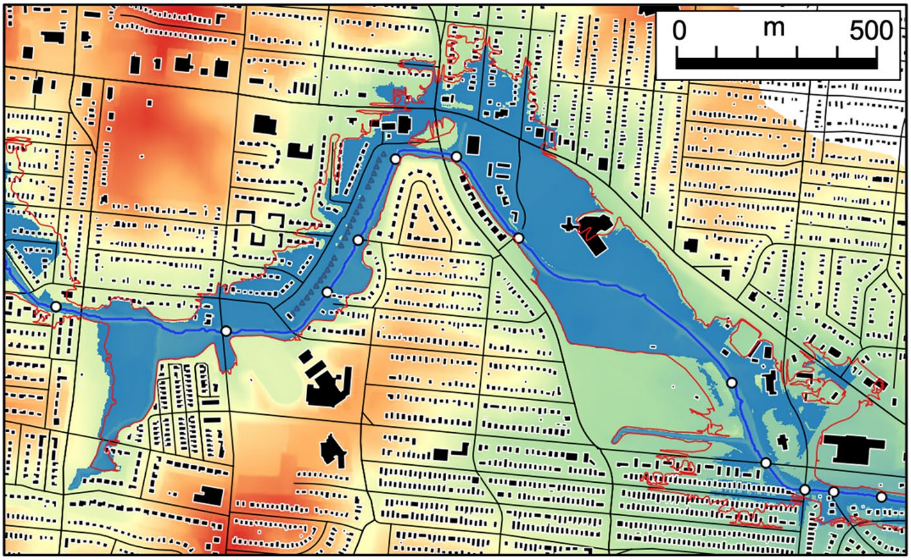

Fig. 5 Area inundated by the 2008 flood (blue shading) along the lower reach of the uRdP, computed with Method 1 processing of measured flood marks (white dots) that were extrapolated a short distance to the uRdP thalweg (solid blue line), on a DEM with color coded elevation (MSDIS, 2021). Black lines are roads (U.S.Census 2021). Dark rectangles are buildings (U.S. Building Footprints 2021); the dark blue Δ's mark former homes that were damaged in 2008 and subsequently demolished after a FEMA buyout (University City 2010). The red line is the border of Zone AE on map 29189C0212K (FEMA 2015)

4.3 2008 flood, upper River des Peres

The flood of 2008 damaged > 200 homes and several businesses in University City. MSD (2013) measured the elevations of three flood marks along the uRdP, which we augmented by using GNSS and total station instruments to determine the elevations of flood marks and water levels recorded in event photographs, plus the level recorded at USGS gauging station 07010022. Figure 5 shows the inundation for the lower reach of the uRdP map computed using Method 1. Two fatalities occurred along this reach, and 28 homes were later demolished following a post-flood federal buyout (Δ's). A spectacular video of the flood taken from one of these former homes is available (YouTube 2008).

4.4 Calculated 10y and 100y flood maps, upper River des Peres

The QGIS raster calculator provides several ways to derive flood maps for different return intervals. The simplest and best method is to use Eq. 1b (Method 1) to modify the elevations of a known flood surface by various additive constants, defined by historical data from a gauging station. As a specific example, analysis (Eq. 7) of data from gauge 07010022 on the uRdp suggest that a "100 year" flood would be 0.57 m deeper than a "10-year" flood, and also that the flood of 2008 approximated a "20 year" flood. Using this information, the areas inundated by hypothetical 10 and 100-year flood floods can

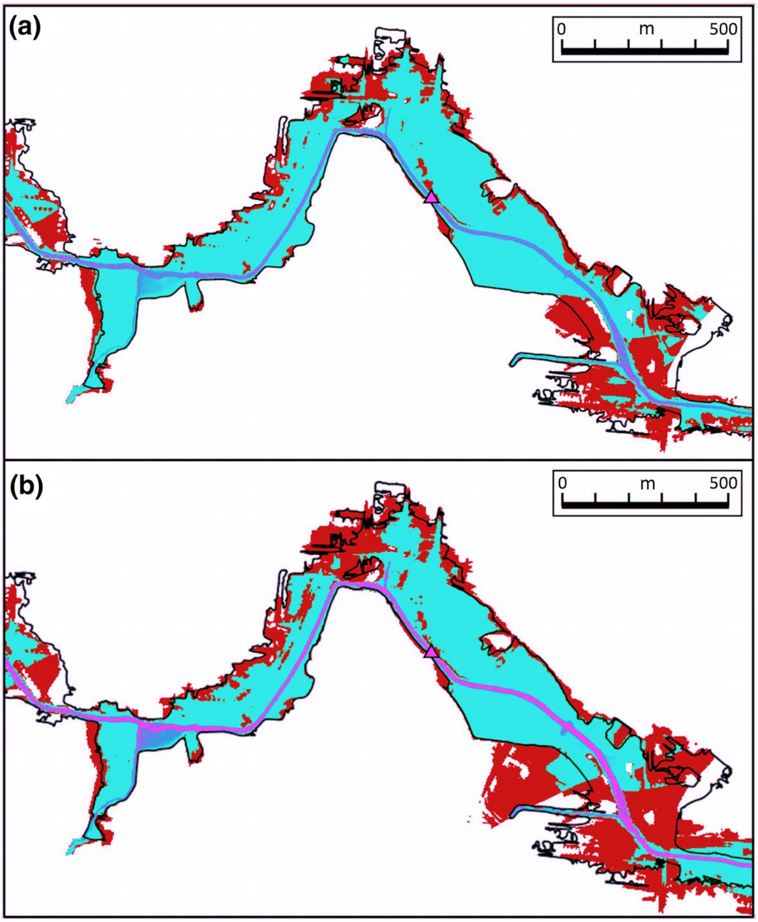

Fig. 6 Maps showing the areas inundated by hypothetical "10-year" (light shading) and "100-year" (dark shading) floods along the lower reach of the uRdP. Also shown are the outline of the FEMA base flood (black line) and the location of gauging station 07010022 (triangle). **a** (top). Flood water surfaces were determined by subtracting 0.17 m, or adding 0.40 m, to the 2008 flood surface shown in Fig. 5. **b** (bottom) Flood water surfaces computed with Method 3, using Eq. 3 with coefficients stated in text, and derived from gauging station data. Differences between our "100-year" area and FEMA Zone AE (black line) tend to increase with distance from the stream gauge, and are largest in flat areas where small differences in water depths greatly affect the lateral extent of shallow water. Note that most of the area inundated by a "100-year" flood is also inundated by a "10-year" flood, which contributes to popular misunderstanding about flood risk

be estimated by subtracting 0.17 m from, or adding 0.4 m to, the measured 2008 flood surface, are shown in Fig. 6a. Good agreement of this "100-year" flood estimate with the FEMA base flood was secured, particularly near the gauge where the statistical difference of 0.4 m was computed.

If a known flood surface is not available, one can be estimated using either Method 2 or 3. Figure 6b provides an example.

5 Discussion

Of all physical quantities, distance is the easiest to accurately measure, and humans have great experience of determining related quantities such as area and position. In contrast, flows and fluxes are complex quantities that are difficult to observe and even harder to quantify. Widespread confusion regarding this point is evidenced by the common use of “flowmeter”. This term is an oxymoron because no available device can measure the flow of a stream; instead, a typical “flowmeter” measures the velocity at a single position in a stream channel, and can do this only if velocity has been properly calibrated against, for example, the rate of rotation of the device’s propeller. Moreover, estimation of streamflow requires that such measurements be made at multiple points across and within a channel, multiplied by measurements of the area of the various channel segments, and the results summed (e.g., Wahl et al. 1995).

Difficulties with discharge estimates are seen in practice. Flows estimated by FEMA and USACE for given water levels are commonly at great odds with USGS rating tables (Criss, 2016). Moreover, USGS rating tables for small streams are mostly based on great extrapolations of measurements at low water levels that have minimal relevance to flooding (Criss and Nelson 2020). Finally, regarding the uRdP in particular, HUD (1978) pointed out that flows estimated by FEMA and USACE for extreme events are probably too large to be conveyed by the tunnel immediately downstream.

Another issue of importance is the effect of bridges on water levels. As shown on thousands of FEMA profiles, HEC-RAS computations commonly depict abrupt drops in water levels immediately downstream of bridges, particularly when the structures are overtopped. While such drops may approximate the condition in the channel, our observations show that overtopping flows at distance from the channel continue to move generally downstream, but sub-parallel to the channel, for 100 m or more, eventually falling back into the channel where the water level is significantly lower. Thus, real measurements of water levels made away from stream channels will represent off-channel flood risk more accurately than any calculation.

Inundation maps can be generated from any real or theoretical elevation profile or water surface. Simple constants or the results of more complex functions can be easily added to any reference surface of interest, using the QGIS raster calculator. The most realistic inundation maps utilize a known reference surface of the mean or some known high water line along the channel, defined by multiple measurements (Fig. 5) or by aerial photographs of flooded areas. Modifications of such surfaces to represent floods of different return intervals are easily made by adding constants to the known surface, using Eq. 1b in the QGIS raster calculator (Fig. 6a). Modifications based on historical high water data provide particularly important insights on flood risk. Volumes of stored floodwater for different water surfaces can also be determined by similar methods that likewise employ the raster calculator. The methodologies developed here can be applied to practically any area, and when the inputs are securely grounded in data, can provide very important insights into flood risk.

If a real flood surface is not available, Methods 2 or 3 can be used to prepare hypothetical inundation maps. Method 2 utilizes only the profile along the thalweg bottom, which provides a useful reference line for small streams that are mostly dry during lidar data acquisition for the DEM. Such hypothetical inundation maps can be improved if QGIS is used to determine the area of the subwatersheds that contribute flow to any point along the thalweg, permitting use of Method 3 (Fig. 6b).

All of the above reasons, plus additional ones discussed by Criss and Luo (2017), suggest that inundation maps, which basically depict water levels, are best computed from actual measurements of water levels, rather than being fundamentally based on discharge estimates and empirical calculations. This paper provides a first attempt to do this. Our early results show promise.

6 Conclusions

Our methodology for inundation mapping utilizes water levels, which are simply and accurately measured, and the long records of stage that are available at thousands of sites. Our conclusions are:

(1) Because inundation maps depict water levels, they can be directly derived from measured flood levels, circumventing the convoluted, intermediary use of discharge estimates.
(2) Inundation maps for actual floods can be determined using purely geometrical relationships, by combining lidar-based DEMs with observed water levels measured at multiple points along or near a thalweg.
(3) Inundation maps for theoretical or statistical floods can be determined by utilizing straightforward theoretical algorithms to estimate water levels, which can be optimized for any particular site.
(4) Data interpolation and the nearest-neighbor gridding algorithm (NNGA) circumvent the necessity of defining specific cross sections.
(5) Freely available software packages can be used to generate inundation maps from measured or computed water levels.

Supplementary Information The online version contains supplementary material available at https://doi.org/10.1007/s11069-022-05270-6.

Author contributions All authors contributed to study conception, design, and manuscript preparation. R.E. Criss collected flood data, developed the mathematical formulae and prepared the manuscript. D.L. Nelson was primarily responsible for implementing the QGIS software, wrote the Excel codes, and prepared the Supplement. All authors read and approved the final manuscript and the supplement, and agree to their submission and publication.

Funding Authors are retired, and received no funding for conducting this study.

Availability of data and material Sources for raster files are provided in text.

Code availability QGIS is open access. The Supplement provides details of our protocols.

Declarations

Conflicts of interest The authors have no relevant financial or non-financial interests to disclose.

References

ASCE (1988) *The River des Peres. A St. Louis Landmark*. Avail at: http://sections.asce.org/stlouis/History/files/River%20des%20Peres%20%20A%20St.%20Louis%20Landmark.pdf

U.S. Building Footprints (2021) Microsoft. https://github.com/Microsoft/USBuildingFootprints. Accessed 4/2021

U.S. Census (2021) Missouri partnership shapefile batch download. https://www.census.gov/geographies/mapping-files/time-series/geo/tiger-line-file.html
Chow VT (1964) Handbook of Applied Hydrology. McGraw-Hill, New York
Criss RE (2016) Statistics of evolving populations and their relevance to flood risk. J Earth Sci 27(1):2–8. https://doi.org/10.1007/s12583-015-0641-9
Criss RE, Luo M (2017) Increasing risk and uncertainty of flooding in the Mississippi River basin. Hydrol Process 31(6):1283–1292
Criss RE, Nelson DL (2020) Discharge-stage relationship on urban streams evaluated at USGS gauging stations, St Louis. Missouri. J Earth Sci 31(6):1133–1141
Criss RE (2022) Dependence of discharge, channel area, and flow velocity on river stage and a refutation of Manning's equation. Geological Society of America Special Paper 553, Ch. 16
FEMA (2015) Flood Insurance Study, St. Louis County, Missouri. Volumes 1–4. Study number 29889CV001A.
FEMA (2020) Flood Map Service Center, various sites and years, avail. at: https://msc.fema.gov/portal/home
Hauth LD, Spencer DW (1971) Floods in Coldwater Creek, Watkins Creek, and River des Peres basins, St. Louis County, Missouri. U.S. Geological Survey Open- File Report 71–106. avail. at: https://pubs.er.usgs.gov/publication/ofr71146
HUD (1978) Flood Insurance Study. City of University City, St. Louis County, Missouri, U.S. Dept. of Housing and Urban Development, p 21p
Leopold LB, Maddock, Thomas (1953) The hydraulic geometry of stream channels and some physiographic implications. U.S. Geological Survey Professional Paper **252**, 57p; avail at: https://pubs.er.usgs.gov/publication/pp252
MSD (2013) High water marks from September 14, 2008 storm. Metropolitan St Louis Sewer District. Personal communication 8/9/2013.
MSDIS (2021) Missouri Spatial Data Information Service. https://data-msdis.opendata.arcgis.com
NOAA (2017) Atlas 14 Point Precipitation Frequency Estimates: Missouri. https://hdsc.nws.noaa.gov/hdsc/pfds/pfds_map_cont.html
NWS (2020a) Advanced Hydrologic Prediction Service. Historic Crests. https://water.weather.gov/ahps2/index.php?wfo=LSX
NWS (2020b) NWS Forecast Office St. Louis, MO https://www.weather.gov/lsx/
Southard RE (2010) Estimation of the magnitude and frequency of floods in urban basins in Missouri. USGS Scientific Investigations Report, SIR 2010-573: 27
Transtrum MK, Machta BB, Brown KS, Daniels BC, Myers CR, Sethna JP (2015) Perspective: sloppiness and emergent theories in physics, biology, and beyond. J Chem Phys 143:010901
University City (2010) Buyout properties, Department of Community Development, Sept, 2010. Avail at: https://patch.com/missouri/universitycity/wilson-avenue-buyouts-underway. Accessed 4 2021
USACE (2004) Upper Mississippi River system flow frequency study: final report. http://www.mvr.usace.army.mil/Portals/48/docs/FRM/UpperMissFlowFreq/Upper%20Mississippi%20River%20System%20Flow%20Frequency%20Study%20Main%20Report.pdf
USACE (2020) Water levels of rivers and lakes. https://rivergages.mvr.usace.army.mil/WaterControl/stationinfo2.cfm?sid
USGS (1981) Guidelines for determining flood flow frequency. Interagency advisory committee on water data, bulletin 17B
USGS (2020a) USGS current water data for Missouri. https://waterdata.usgs.gov/mo/nwis/rt. Accessed Feb. 2020a
USGS (2020b) Peak streamflow for the nation. http://nwis.waterdata.usgs.gov/usa/nwis/peak. Accessed Feb. 2020b
USGS (2020c) 3DEP lidar explorer. https://prd-tnm.s3.amazonaws.com/LidarExplorer/index.html#/. Accessed Feb. 2020c
Vineyard JD (1967) Physiography, mineral and water resources of Missouri, Missouri division of geological survey and water. Resources 43:13–15
Wahl KL, Thomas WO Jr, Hirsch RM (1995) Stream-gaging program of the US Geological Survey. US Geol. Survey Circular 1123. http://water.usgs.gov/pubs/circ/circ1123/
Wilson DA (2009) Hurricane Ike and impact of localized flooding in St Louis County. In: Criss RE, Kusky TM (eds) inding the balance between floods, flood protection, and river navigation. St. Louis University, Center for Environmental Sciences, St. Louis, pp 22–27
Winston WE, Criss RE (2016) Dependence of mean and peak streamflow on basin area in the conterminous United States. J Earth Sci 27(1):83–88
YouTube (2008) University city flood. https://www.youtube.com/watch?v=9-O3ymI4O48